

# Effect of Plain Flap Over the Aerodynamic Characteristics of Airfoil NACA 66-015

Imanbir Singh  
garrybabbar.gb@gmail.com

**Abstract :-** Effect of plain flap on the distribution over the symmetrical aerofoil NACA 66-015. Flap is a sub-control surface that enhances the lift of the aircraft. This paper includes placing of NACA 66-015 aerofoil with trailing edge flaps at a constant Reynolds number. Measurement of coefficient of pressure ( $C_p$ ) over the aerofoil at different angle of attacks, different flap settings have been done. An investigation on performance of aerofoil with flap has been done to understand the pressure distribution over and below the wing. Laser illuminated smoke visualization have been used to identify flow separation point. It was observed that the stall angle increased and performance of the wing was more enhanced as the angle of attack increased. ANSYS FLUENT analysis to validate experimental results.

## I. INTRODUCTION

An airfoil or aerofoil is the shape of a wing, blade (of a propeller, rotor, or turbine), or sail (as seen in cross-section). An airfoil-shaped body moved through a fluid produces an aerodynamic force. The component of this force perpendicular to the direction of motion is called lift. The component parallel to the direction of motion is called drag. Subsonic flight airfoils have a characteristic shape with a rounded leading edge, followed by a sharp trailing edge, often with a symmetric curvature of upper and lower surfaces. Foils of similar function designed with water as the working fluid are called hydrofoils.

The lift on an airfoil is primarily the result of its angle of attack and shape. When oriented at a suitable angle, the airfoil deflects the oncoming air (for fixed-wing aircraft, a downward force), resulting in a force on the airfoil in the direction opposite to the deflection. This force is known as aerodynamic force and can be resolved into two components: lift and drag. Most foil shapes require a positive angle of attack to generate lift, but cambered airfoils can generate lift at zero angle of attack. This "turning" of the air in the vicinity of the airfoil creates curved streamlines, resulting in lower pressure on one side and higher pressure on the other. This pressure difference is accompanied by a velocity difference, via Bernoulli's principle, so the resulting flow field about the airfoil has a higher average velocity on the upper surface than on the lower surface. The lift force can be related directly to the average top/bottom velocity difference without computing the pressure by using the concept of circulation and the Kutta- Joukowski theorem.

## A. The Selected Airfoil

The aerofoil is NACA66015 where the first number represents the design co-efficient of lift i.e.

$$\frac{3}{20} * 6 = 0.9 \quad \dots \dots (1)$$

the second number represents the position of maximum camber in terms of cord length.

$$\frac{1}{20} * 6 = 0.3 \quad \dots (1.2)$$

which is at 30% of the cord length, the third number represents that it has a normal camber line which means it is a symmetrical airfoil, the fourth and fifth number represents that it has maximum thickness of 15% of the cord.



Fig 1.1. wing section with aerofoil NACA 66015

## B. FLAPS

Flaps are a type of high-lift device used to increase the lift of an aircraft wing at a given airspeed. Flaps are usually mounted on the wing trailing edges of a fixed-wing aircraft. Flaps are used to lower the minimum speed at which the aircraft can be safely flown, and to increase the angle of descent for landing. Flaps also cause an increase in drag, so they are retracted when not needed. Extending the wing flaps increases the camber or curvature of the wing, raising the maximum lift coefficient or the upper limit to the lift a wing can generate. This allows the aircraft to generate the required lift at a lower speed, reducing the stalling speed of the aircraft, and therefore also the minimum speed at which the aircraft will safely

maintain flight. The increase in camber also increases the wing drag, which can be beneficial during approach and landing, because it slows the aircraft. In some aircraft configurations, a useful side effect of flap deployment is a decrease in aircraft pitch angle, which lowers the nose thereby improving the pilot's view of the runway over the nose of the aircraft during landing. In other configurations, however, depending on the type of flap and the location of the wing, flaps can cause the nose to rise (pitch-up), obscuring the pilot's view of the runway.

In our case it is a plain flap with 15 degrees of allowance both in positive and negative direction. The effect of the flap is studied with the help of the graphs which will show us the lift difference that would be encountered when we change the flaps and will tell us the arrangements of the flaps which would be beneficial for us and which would increase the drag of the airfoil.

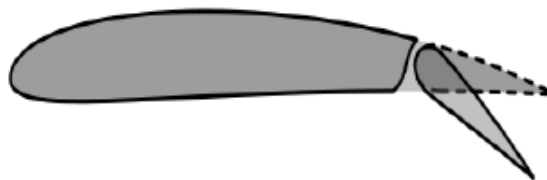


Fig.1.2. airfoil with the plain flap in positive direction

*C. Undertaking*

1. Measurement of coefficient of pressure (Cp) over the airfoil at different angle of attacks, different flap settings have been done in the wind tunnel.
2. Plotting of graphs for all possible angle of attacks with combination of flap angles are done.
- 3 Laser illuminated smoke method and oil visualization was done on the model.

*D. Why this Work Undertaken*

1.The aerodynamic performance of an air-foil can be best understood by the variation of pressure over it as the pressure difference can be directly related to the lift generated or the lift difference in the field. This distribution is expressed in terms of the pressure coefficient.

$$c_p = \frac{P - P_a}{\frac{1}{2} \rho v^2} \dots \dots (1.3)$$

where,

- C<sub>p</sub> = co-efficient of pressure
- P = pressure value at that particular port in bar
- P<sub>a</sub> = ambient pressure value in bar
- ρ = density of the air in kgm<sup>3</sup>/
- V = Velocity of the air in m/s

2. Since the pressure distribution over an air-foil without flaps is an important characteristic to be understood an attempt was made to explore the pressure distribution over a wing with flaps. So, this attempt lead us to the study of the airfoil with flaps and what changes occur when the flaps are introduced.

3. For this, variation of pressure over an air-foil (cross section of a wing) NACA 66015, which is unexplored was studied.

**II. EXPERIMENTAL SETUP AND APPARATUS**

*A. Introduction*

Construction of a wind tunnel airfoil model with a trailing edge flap was performed. The model is instrumented in order to measure pressure heads. It is used to calculate coefficient of pressure (Cp). The related description of the equipment used in this experiment is provided in the following sections.

*B. Apparatus*

▪ *Wind Tunnel*

The Wind Tunnel used is a subsonic, an open-circuit blow down low-speed tunnel. A schematic drawing is shown in Figure 2.1, for inlet flow turbulence control one honeycomb and five nylon flow conditioning screens are included in the settling chamber. The test section is 45cm x 30cm , having a working area with an easily removable glass wall in the side for convenient tunnel access and visualization. The top wall is also made of Plexiglas to accommodate light sources for use in flow visualization.

• *Aerofoil Model*

The model section is a symmetrical aerofoil NACA 66-015 with trailing edge flap. The chord length is 15cm resulting in an airfoil maximum thickness of 2.25cm. The airfoil has 24 pressure ports which is connected to tubes. These tubes are connected to a pressure scanner and it is used to measure the pressure at different ports.



Fig 2.1 subsonic wind tunnel



Fig 2.2. NACA 66-015 Aerofoil



Fig 2.3. pressure port on aerofoil

- *Pressure Scanner*

A digital manometer pressure scanner with 64 ports is used for the project. The pressure ports of the airfoil is connected to a digital pressure scanner which gives pressure head readings and also the  $h_0$  and  $h_{\infty}$ . These readings are used to calculate the  $C_p$  value, which later plotted.



Fig 2.4. pressure scanner

### C. Experiment

1. Place the NACA 66-015 aerofoil in the subsonic wind tunnel
2. Connect all the pressure ports on the aerofoil to the pressure scanner
3. Take wind-off readings while the tunnel is switched off
4. Switch on the tunnel with velocity of 10 m/s
5. Take pressure head readings at various angle of attacks and flap angles.
6. Using the formula, calculate the coefficient of pressure ( $C_p$ ) and plot respective graphs and analyses stall angle.

## III. EXPERIMENTAL EVALUATION

### A. Calculation of $C_p$

The wind tunnel experiment gave us the value of the pressure head denoted by  $h$ . The  $C_p$  value can be calculated by the formula.

$$C_p = \frac{h - h_\infty}{h_0 - h_\infty} \dots \dots (1.4)$$

where,

h = is the static pressure head at the point at which pressure coefficient is being evaluated.

h<sub>∞</sub> = is the static pressure head in the free stream.

h<sub>0</sub> = is the stagnation pressure head in the free stream.

The values of h<sub>∞</sub> and h<sub>0</sub> were evaluated at the beginning of every experiment. The h value was then measured at each port on the aerofoil and then the C<sub>p</sub> value was calculated for the particular angle of attack and flap angle.

• *Tabulation of The CP Values*

The values of C<sub>p</sub> for each angle of attack and the respective flap angle was entered in MS Excel.

This tabulation was helpful in order to plot the graphs between C<sub>p</sub> and the location of port.

The table involves the values of C<sub>p1</sub> , C<sub>p5</sub> at each deflection of angle of attack and the flap angle and the location of port.

The following figures shows the values of C<sub>p</sub> after calculations. In these tables the value of flap angle has been changed when the aerofoil was kept at a fixed angle of attack.

distance	distance	Cpu0	Cpl0	Cpu5	Cpl5	Cpu10	Cpl10	Cpu15	Cpl15
0		0.74	0.9	0.644	0.944	0.538	0.825	0.274	0.65
1.5		-1.86	0.315	-2.106	0.278	-2.291	0.45	-2.35	0.68
3		-1.61	0.21	-1.829	0.182	-1.949	0.36	-2.309	0.574
6	6	-1.306	0.505	-1.431	0.536	-1.542	0.615	-1.782	0.708
12	12	-0.582	0.233	-1.246	0.285	-1.387	0.378	-1.562	0.484
22.5	22.5	-0.909	0.097	-1.034	0.185	-1.034	0.252	-1.477	0.356
40.5	40.5	-0.715	-0.166	-0.793	-0.107	-1.494	-0.001	-0.866	0.116
58.5	58.5	-0.663	-0.254	-0.701	-0.183	-0.682	-0.063	-0.738	0.0789
78	78	-0.79	-0.345	-0.886	-0.294	-0.987	-0.109	-0.847	0.087
97	97	-0.409	-0.421	-0.263	-0.405	-0.389	-0.183	-0.459	-0.285
117	117	-0.286	-0.045	-0.401	-0.129	-0.402	-0.183	-0.44	-0.067
135	135	-0.294	0.45	-0.451	-0.017	-0.543	-0.105	-0.59	-0.079
150		0.018		-0.183		-0.412		-0.412	

Fig 3.1 angle of attack 3

distance	Cpu0	cpl0	cpu5	cpl5	cpu10	cpl10	cpu15	cpl15
0	0.3524	0.3524	0.15	0.2158	-0.1	0.003	-0.317	-0.185
1.5	-2.3302	0.821	-2.263	0.888	-2.217	0.9427	-2.309	0.97
3	-2.2371	0.785	-2.291	0.8182	-2.198	0.898	-2.251	0.95
6	-1.7752	0.6854	-1.893	0.734	-2.124	0.832	-2.217	0.879
12	-1.556	0.4449	-1.29	0.484	-1.659	0.592	-1.89	0.675
22.5	-1.4051	0.2599	-1.755	0.343	-2.023	0.436	-2.152	0.527
40.5	-0.8501	-0.01757	-0.826	0.037	-0.865	0.169	-0.865	0.274
58.5	-0.7206	-0.2025	-0.682	-0.073	-0.713	0.106	-0.71	0.237
78	-0.8501	-0.295	-0.83	-0.202	-0.978	0.035	-1.388	0.219
97	-0.3876	-0.3876	-0.497	-0.328	-0.425	-0.196	-0.266	-0.328
117	-0.2957	0.000925	-0.361	-0.133	-0.387	-0.067	-0.414	0.012
135	-0.1639	0.0286	-0.346	-0.079	-0.369	-0.045	-0.5165	-0.013
150	-0.0175		-0.332		-0.359		-0.385	

Fig 3.2 angle of attack 6

distance	cpu0	cpl0	cpu5	cpl5	cpu10	cpl10	cpu15	cpl15
0	-0.3133		-0.212	-0.652	-0.341	-0.695	-0.035	-0.257
1.5	-2.2833		-2.189	0.979	-2.097	0.979	-1.4479	0.9633
3	-2.2363		-2.152	1.0318	-2.078	1.0138	-1.547	1.004
6	-2.2457	0.8536	-2.106	0.841	-2.04	0.893	-1.39	0.881
12	-2.21	0.6247	-2.187	0.616	-1.95	0.682	-1.3255	0.657
22.5	-2.1894	0.4371	-2.075	0.527	-1.99	0.514	-1.449	0.5
40.5	-0.923	0.0806	-0.8	0.129	-0.849	0.22	-1.205	0.22
58.5	-0.7354	-0.03189	-0.65	0	-0.655	0.138	-1.03	0.225
78	-1.5328	-0.2195	-1.38	-0.149	-1.727	0.035	-1.4	0.176
97	-0.913	-0.3789	-0.198	-0.328	-0.307	-0.209	-0.806	-0.513
117	-0.2945	-0.0787	-0.374	-0.12	-0.401	-0.066	-0.618	-0.083
135	-0.228	-0.03189	-0.452	-0.063	-0.495	-0.052	-0.704	-0.122
150	-0.1632		-0.341		-0.372		-0.581	

Fig 3.3. angle of attack 9

distance	cp0	cpl0	cp5	cpl5	cpu10	cpl10	cpu15	cpl15
0	0.3256	0.3256	0.4	-0.029	0.331	0.0061	0.335	0.0031
1.5	-1.0712	-1.0712	-0.815	0.963	-0.786	0.963	-0.786	0.963
3	-1.0231	-1.0231	-0.757	0.963	-0.747	0.963	-0.747	0.998
6	-0.9267	0.8073	-0.766	0.79	-0.737	0.823	-0.718	0.803
12	0.5664	0.5664	-0.951	0.553	-0.851	0.599	-0.791	0.6608
22.5	-0.8786	0.3737	-0.766	0.39	-0.747	0.46	-0.742	0.462
40.5	-1.02312	0.0366	-0.796	0.072	-0.761	0.17	-0.786	0.178
58.5	-0.8304	-0.156	-0.766	-0.068	-0.766	0.091	-0.766	0.097
78	-1.02312	-0.3487	-0.825	-0.227	-0.796	-0.015	-0.805	0.009
97	-0.6377	-0.6377	-0.871	-0.68	-0.871	-0.62	-0.911	-0.63
117	-0.6377	-0.2042	-0.659	-0.238	-0.669	-0.181	-0.669	-0.168
135	-0.15606	-0.15606	-0.686	-0.238	-0.715	-0.208	-0.715	-0.191
150	-0.493		-0.643		-0.657		-0.64	

Fig 3.4 angle of attack 12

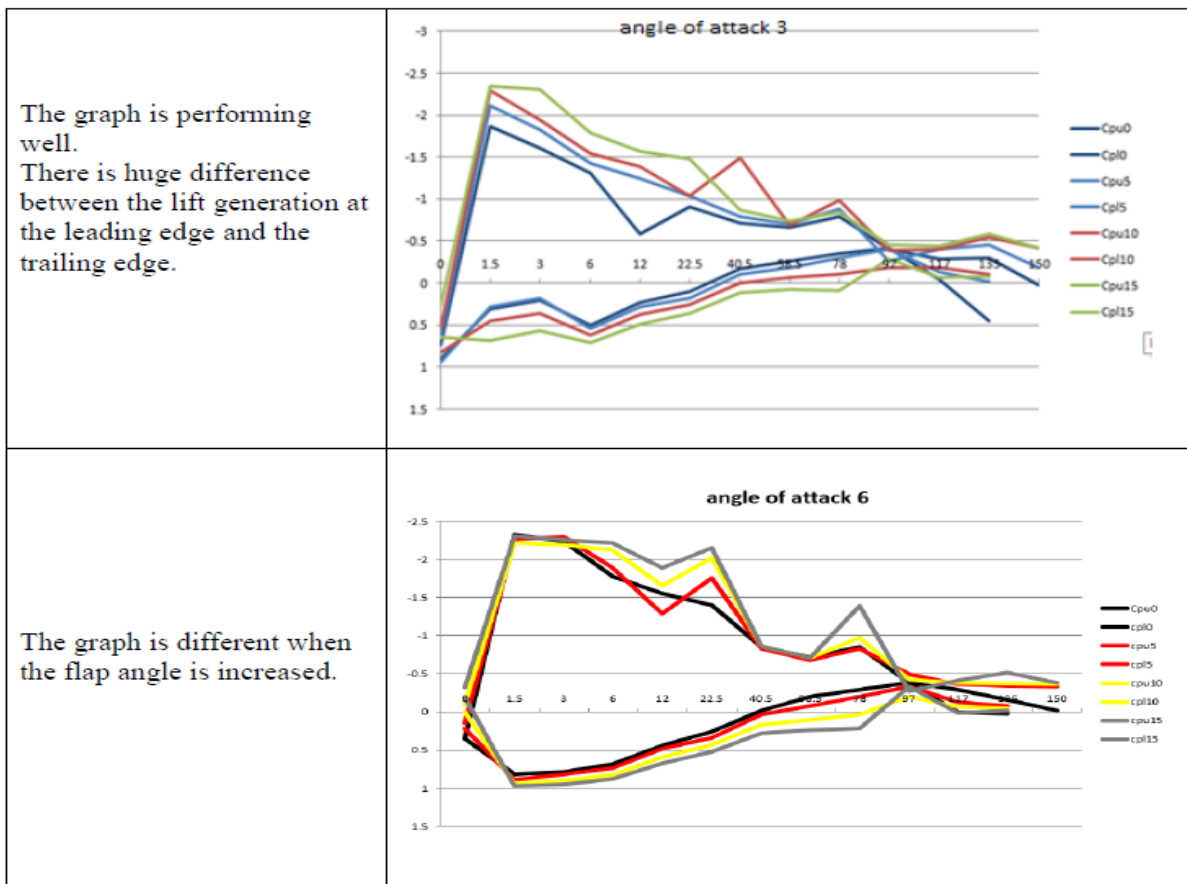
ditance	distance	Cpu0	Cpl0	Cpu5	Cpl5	Cpu10	Cpl10	Cpu15	Cpl15
0		0.3581	0.3581	0.258	0.003	0.199	-0.046	0.041	-0.
1.5		-0.6582	-0.6582	-0.76	0.959	-0.747	0.973	-0.823	0.96
3		-0.6582	-0.6582	-0.688	0.983	-0.708	0.973	-0.74	0.99
6	6	-0.6582	0.8131	-0.698	0.852	-0.684	0.862	-0.783	0.9
12	12	-0.6001	0.6001	-0.78	0.638	-0.78	0.686	-0.78	0.74
22.5	22.5	-0.6582	0.4065	-0.708	0.481	-0.698	0.52	-0.783	0.58
40.5	40.5	-0.7066	0.01936	-0.718	0.136	-0.727	0.208	-0.823	0.31
58.5	58.5	-0.6582	-0.1742	-0.718	-0.015	-0.727	0.101	-0.823	0.21
78	78	-0.6962	-0.4162	-0.747	-0.21	-0.755	-0.044	-0.854	0.18
97	97	-0.6582	-0.6582	-0.997	-0.762	-0.983	-0.542	-0.997	-0.8
117	117	-0.7066	-0.3194	-0.688	-0.179	-0.669	-0.191	-0.762	-0.
135	135	-0.6824	-0.271	-0.75	-0.25	-0.75	-0.191	-0.77	-0.17
150		-0.6582		-0.649		-0.64		-0.759	

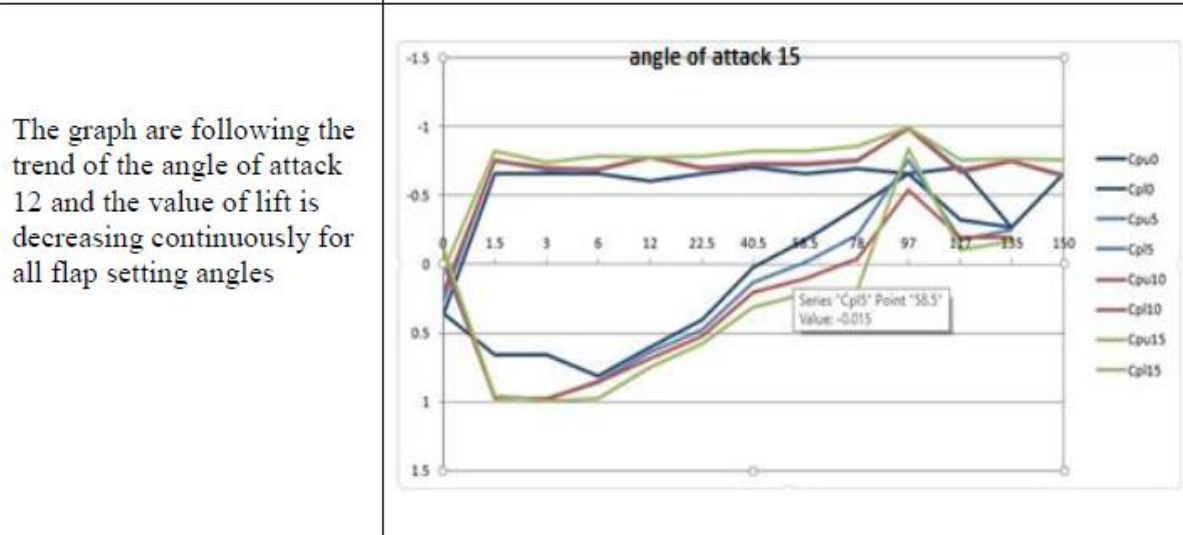
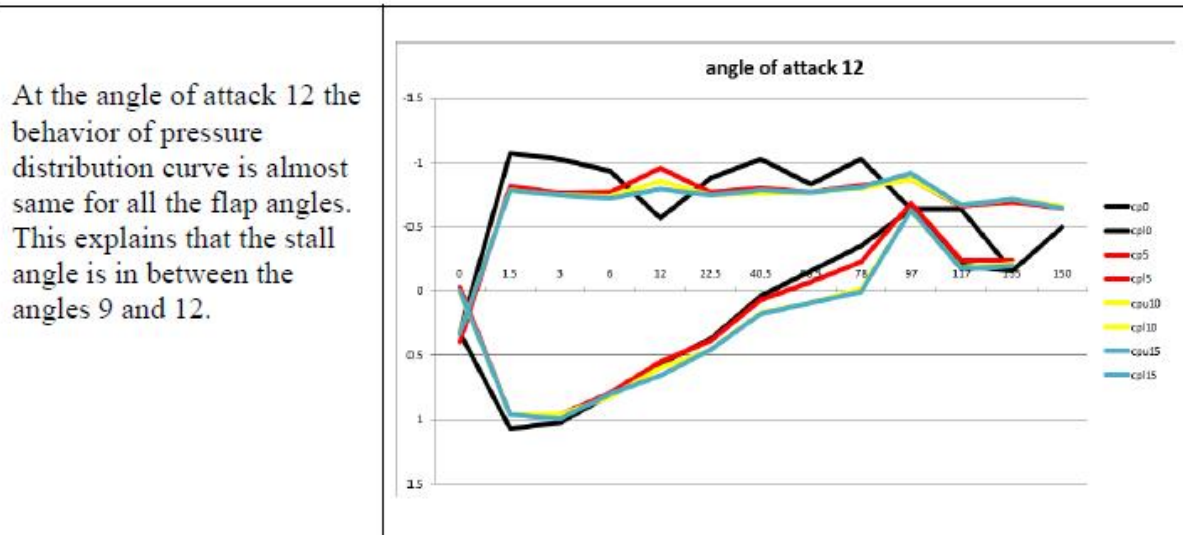
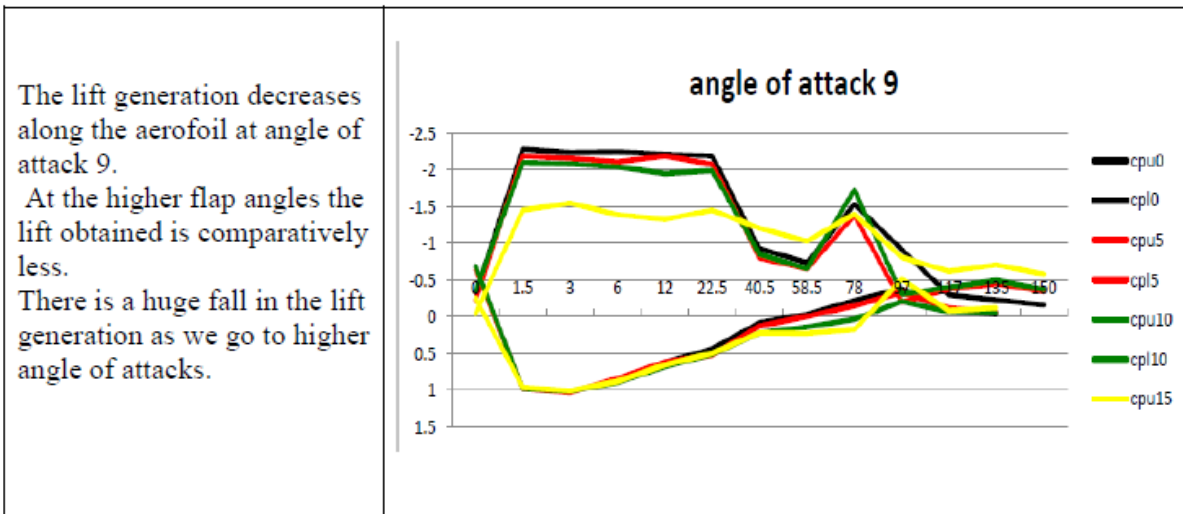
Fig 3.5 angle of attack 15

distance	CPu0	Cpl0	cpu5	Cpl5	Cpu10	Cpl10	Cpu15	Cpl15
0	0.0975	0.0975	-0.06	-0.074	-0.133	-0.146	-0.263	-0.28
1.5	-0.7317	-0.7317	-0.793	0.958	-0.772	-0.958	-0.803	0.958
3	-0.6829	-0.6829	-0.752	0.984	-0.772	0.984	-0.783	0.99
6	-0.7024	0.87	-0.752	0.917	-0.752	0.927	-0.783	0.958
12	0.68229	0.68229	-0.797	0.751	-0.766	0.795	-0.766	0.856
22.5	-0.6829	0.439	-0.742	0.566	-0.722	0.601	-0.803	0.673
40.5	-0.7219	0.0975	-0.793	0.215	-0.793	0.288	-0.823	0.408
58.5	-0.7317	-0.0975	-0.813	0.058	-0.793	0.13	-0.844	0.296
78	-0.7219	-0.3902	-0.813	-0.164	-0.823	0	-0.823	0.214
97	-0.7804	-0.7804	-1.11	-0.84	-1.055	-0.637	-1.055	-0.925
117	-0.7804	-0.3707	-0.747	-0.262	-0.762	-0.202	-0.783	-0.77
135	-0.3414	-0.3414	-0.838	-0.273	-0.78	-0.253	-0.807	-0.189
150	-0.7219		-0.747		-0.745		-0.759	

Fig 3.6 angle of attack 18

Table. 3.1 Result of the following values in terms of graphs were plotted and analyzed





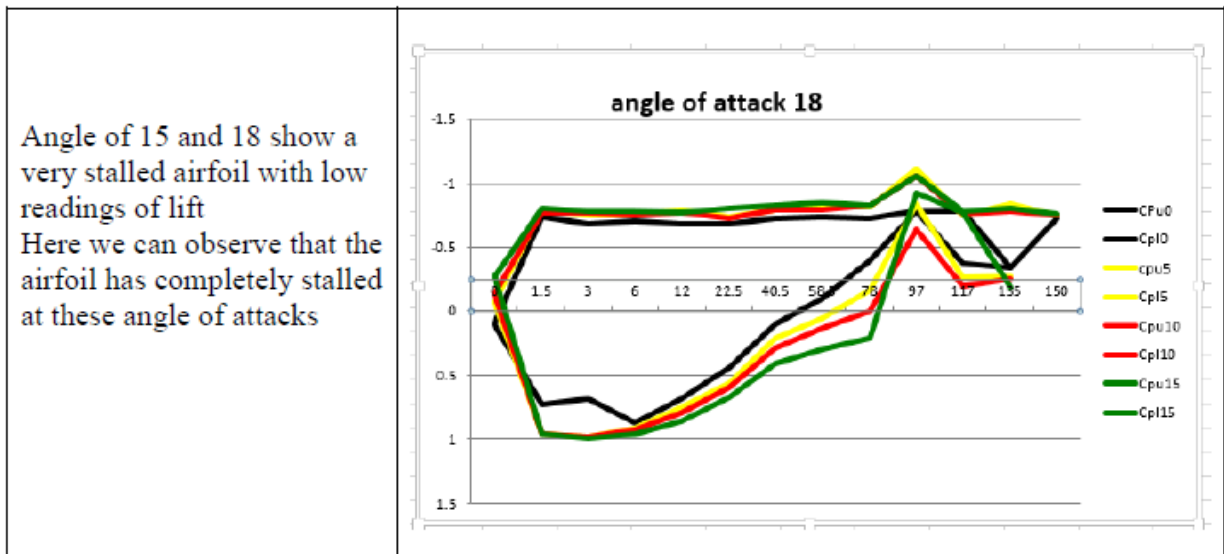
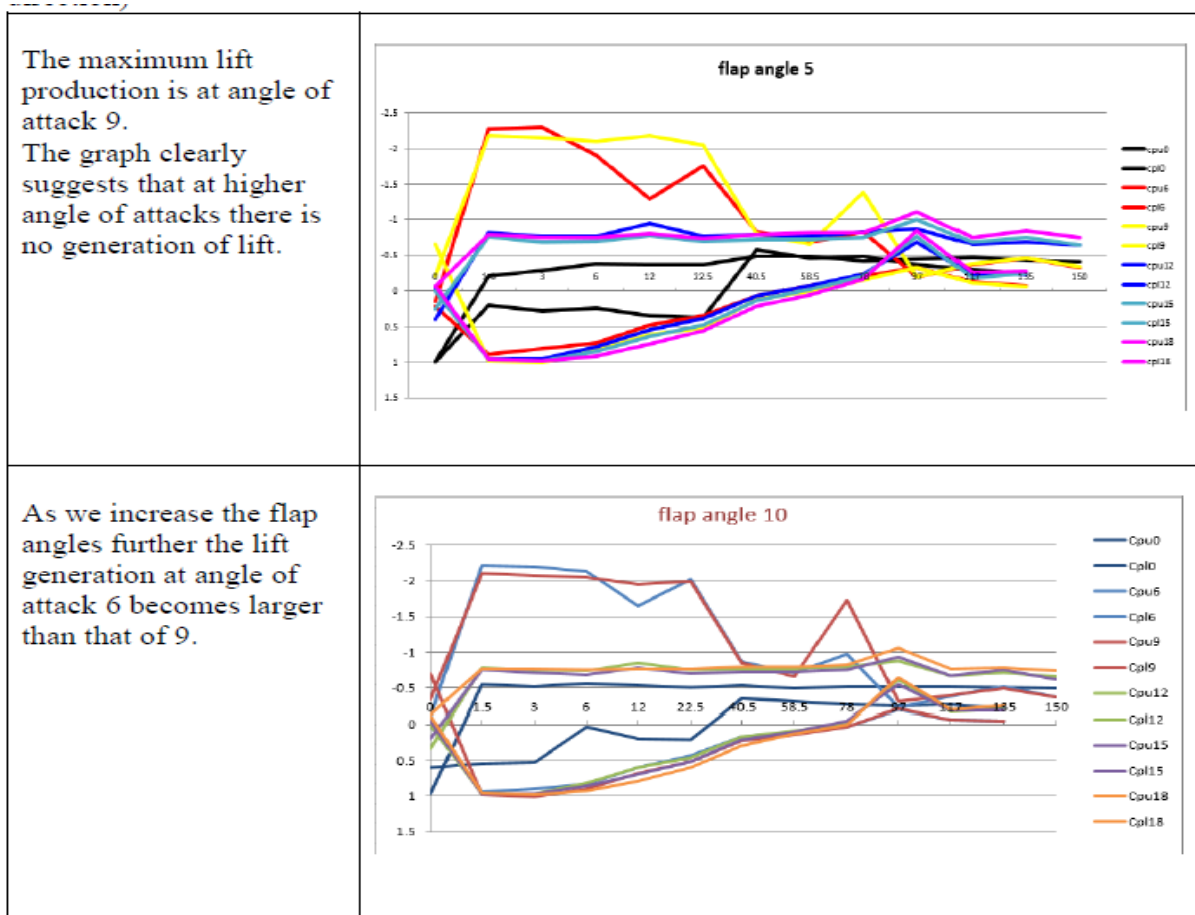
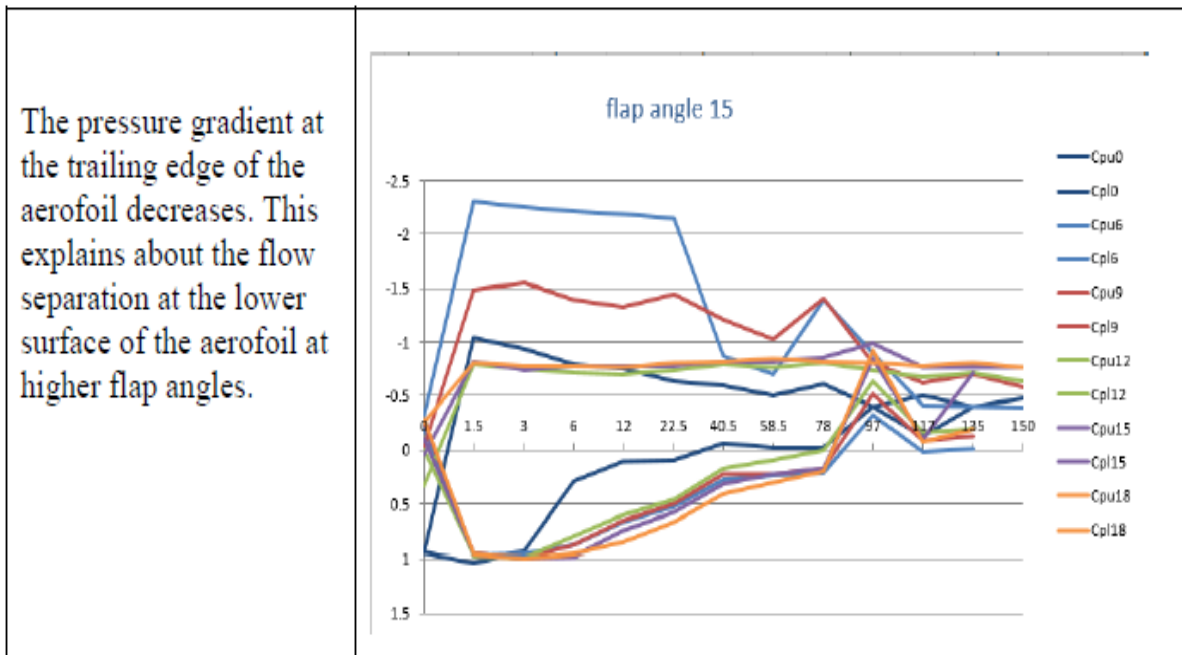


Table. 3.2 The graphs when the angle of attack is changed in the positive direction (upward direction)





#### IV. SMOKE VISUALISATION

##### A. Introduction

Flow visualization or flow visualization in fluid dynamics is used to make the flow patterns visible, in order to get qualitative or quantitative information on them. Unlike other techniques, which are limited to measuring flow conditions at discrete points within the flow field, flow visualization techniques are capable of yielding a qualitative macroscopic picture of the overall flow field.

##### B. Experimental

The experiments were performed in a subsonic type wind tunnel. Hot-wire anemometry (HWA) measurements across the test section of the wind tunnel showed a uniform free-stream and a turbulence.

The experiments were performed to determine the smoke fluid, voltage and lighting arrangement to produce the best result for smoke-wire apparatus. Since the apparatus would be in the tunnel, an oil delivery system had to be designed for continuous operation. An oil reservoir was placed on the top of the nozzle-settling chamber, which was the same height as the test section roof. A tube was used to supply air from the air supply gauge while another tube was used to transport smoke fluid to the heating wire inside the test section. The principal of oil delivery system was based on the gravitational potential energy. There were lighting arrangements suggested to produce clearer images for image recording. The main problem in recording the smoke lines was reflection of image in the Perspex of the test section wall.



Fig. 4.1 Angle of attack 9 with flap at five degrees

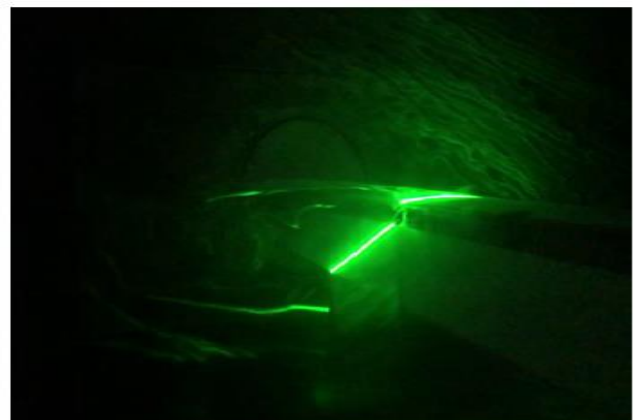


Fig. 4.2 Angle of attack 15 with flap at 15 degrees





Fig.4.3 Angle of attack 12 with flap at 10 degrees

### C. Results and Discussion

The fluid, which has higher boiling flow rate, will certainly give better smoke wire visibility at high speed. It was found that the paraffin produced better results than other smoke fluids. Clear, uniform and long duration smoke lines were generated by using two- and three-coiled copper wires at wind tunnel velocity of 10 m/s respectively. Moreover, paraffin is a non-irritant, nonflammable and non-hazardous liquid. Gasoline could also be used but it is a highly flammable liquid. The best voltage to use with these wires depends on the tunnel velocity, but is generally around 10 to 12 V. At high

velocity, forced convection effect becomes dominant and the wire needs more energy to surpass the smoke fluid boiling point. Loss in energy due to resistance is balanced with the heat generation. Assuming the temperature coefficient is small, total resistance is only dependent on length of the wire, resistivity of the material, and the wire cross-sectional area are small. Copper wire releases more heat compared to stainless steel. Due to low electrical resistance, steel wires release less heat to be absorbed by the smoke fluids. Smaller diameter of copper wire has higher resistance, lower in heat loss through convection and generates higher boiling rate. Since copper dissipates the highest amount of heat, it is very suitable as a heating element. Since both the two- and three-coiled copper wires can generate good quality smoke lines using the paraffin smoke liquid, further experiment was performed to capture the smoke generated from those wire designs. From the results, two-coiled copper wire design was chosen for this smoke-wire apparatus since it generates clear, uniform white dense smoke and easy attachment of the liquid to the wire. The photograph of the smoke generated, as shown in above confirms this. Evolution of the vortex structure is clearly shown. The application of top and side lighting arrangements gives sufficient illumination and reduce reflection of image in the Perspex of the test section wall for photographic purposes using digital camera. Higher heat capacity and higher latent heat of vaporization cause water needs more heat to surpass boiling point for generating smoke. - Palm oil No smoke is generated by using two- and three-coiled copper wires. Diesel Light smoke is generated by using three-coiled copper wire. Clear and uniform smoke is generated by using two coiled copper wire but in short duration. The odor of diesel is spread in the lab. Gasoline Clear and uniform smoke is generated. The odor of gasoline is spread in the lab. Corn oil No smoke is generated by using two- and three-coiled wires. Paraffin Clear and uniform smoke is generated by using two- and three-coiled wires at voltage. No odor is generated due to the smoke. So here we clearly can see that as the angle of attack increased from 9 to 12 there is a huge difference in lift and as we increase the flap angle the stall can be delayed

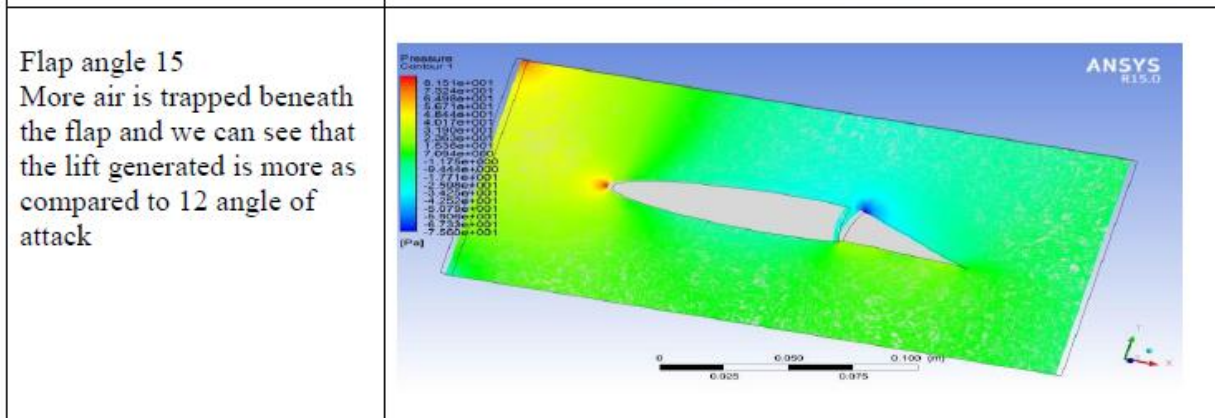
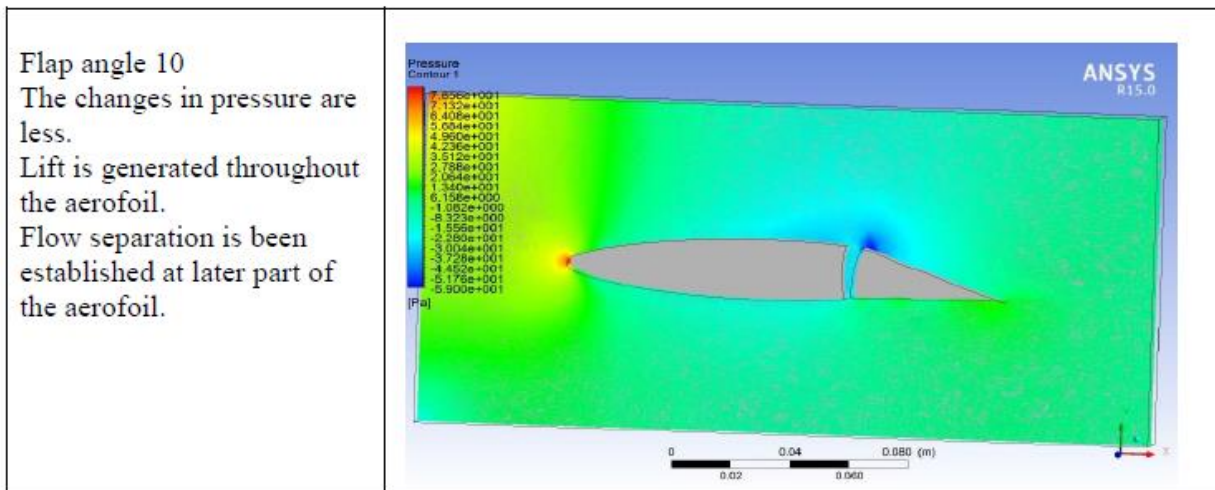
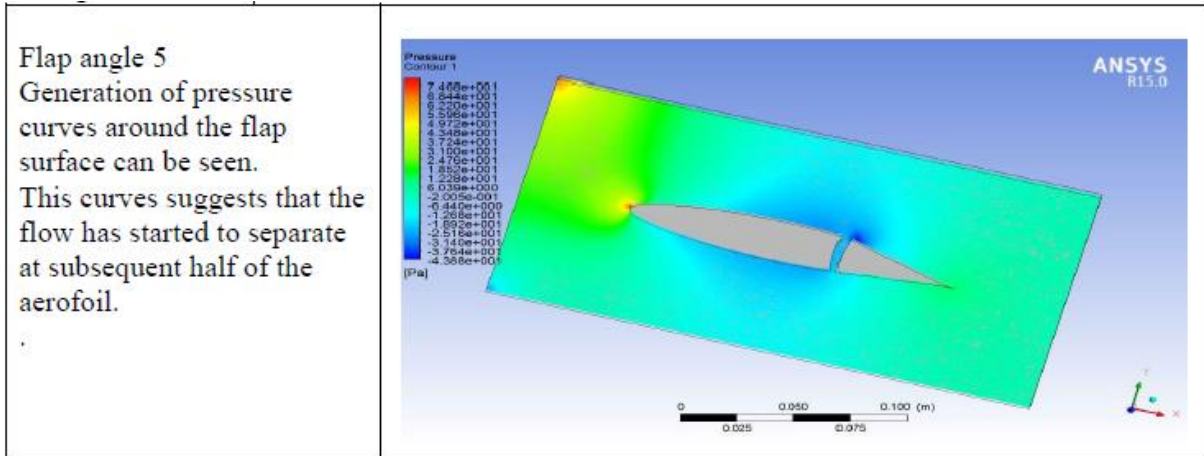
## V. COMPUTATIONAL ANALYSIS

### A. Computational Analysis For Our Project

The computational analysis of our project is achieved with the help of the computational fluid dynamics which is achieved with the help of ANSYS FLUENT 15.0.

In this software we input our designed model in our case the airfoil as a replica of the model. This is designed with the help of CATIA designing software, then it is imported in the ansys software.

The below table 5.1 gives the observation of the changes happening when the flap is changed at angle of attack 9.



The below table 5.2 gives the observation of the changes happening when the flap angles are changed at the angle of attack 12.

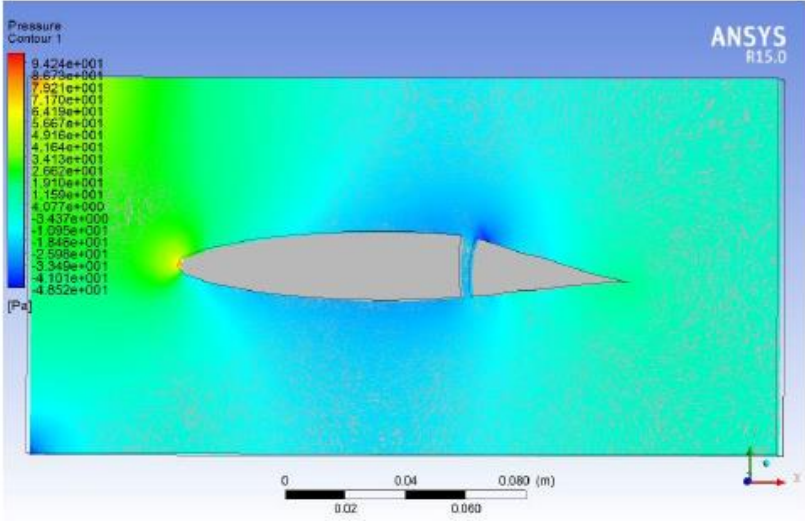
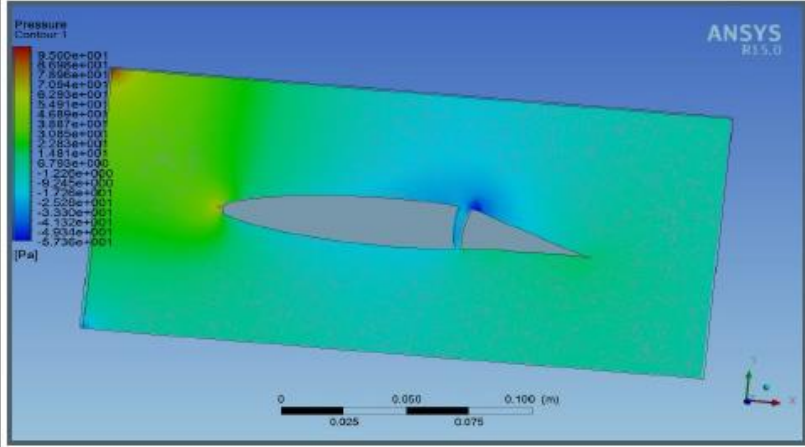
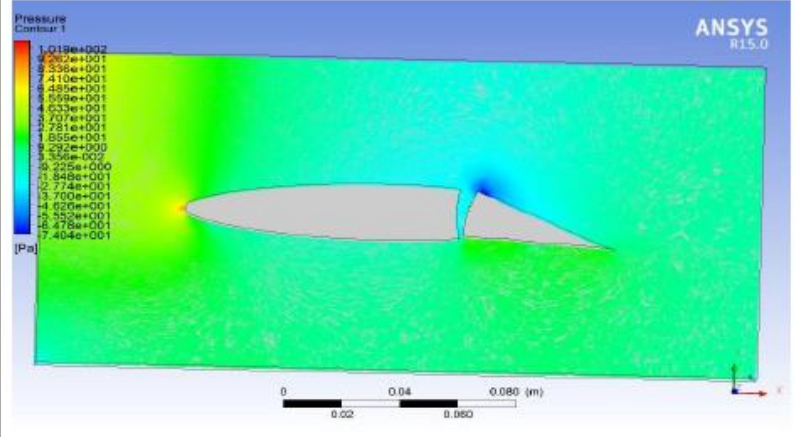
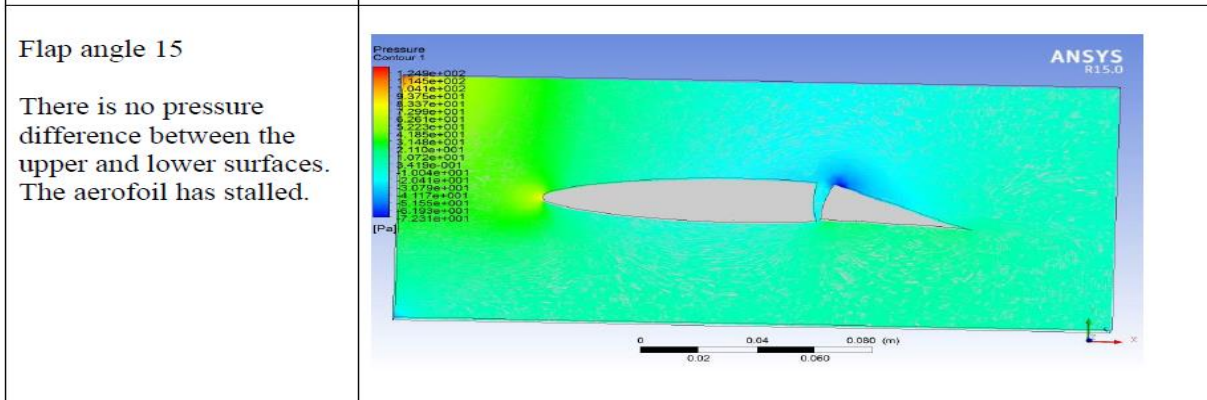
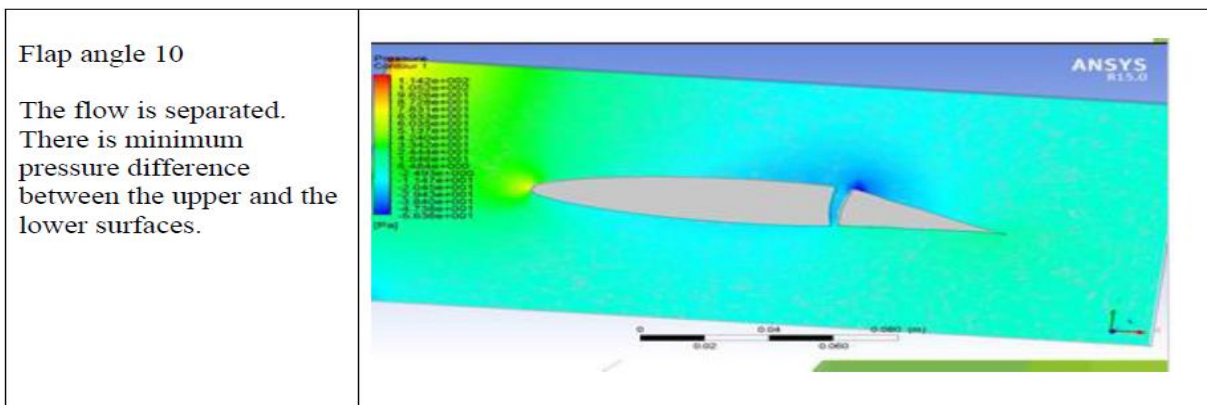
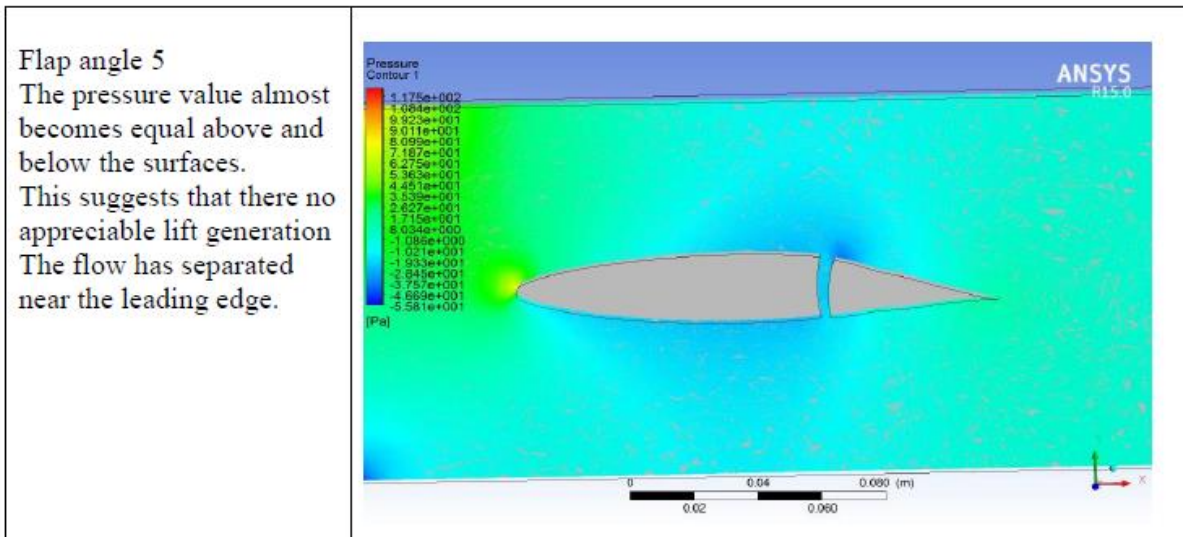
<p><b>Flap angle 5</b>                  This result shows that the pressure value abruptly changes to a high value somewhere past the leading edge of the aerofoil.                  The flow separation has taken place and the lift generation is decreased as we move towards the flaps.</p>	
<p><b>Flap angle 10</b>                  At angle of attack 12 the pressure curve has been increased.                  The lift generation is less than previous case.</p>	
<p><b>Flap angle 15</b>                  There is no pressure difference between the upper and lower surfaces.                  The aerofoil has stalled</p>	

Table 5.3 Below is table for angle of attack 15.



From these tables we can easily observe that the there is a great stall produced as we go from angle of attack 9 to 12 and due to the effects of flaps our lift is getting delayed

**VI. RESULT AND CONCLUSION**

The aerofoil without flap gives us a stable and optimum amount of lift at both upper and lower surface of the aerofoil, this is the best orientation for an aerofoil to cruise.

As the flaps are deflected at the negative direction, with the positive deflection in angle of attack, the pressure gradient curve around the aerofoil suggested the change in the behavior of the fluid flow across the aerofoil cross section.

It was observed that the pressure at the leading edge decreases as we increase the angle of attack. At the trailing edge the pressure at the lower surface shows drastic changes.

Larger the deflection in flap, more the flow is trapped beneath the airfoil, leading to decrease of flow velocities and build-up of the pressure below the airfoil. Simultaneously, the increasing adverse pressure gradient with flap deflection yields a larger flow separation behind the flap.

The flow separation starts at the angle of attack 9 and gets completely stalled by 15 and 18 angles. Though this paper wont be that much effective in the advancement of aerodynamics but this paper can be o great significance to a person or group who wants to experiment with some similar airfoil and wants to use it to innovate something else.

### REFERENCES

- [1]. Shubham Maurya Pressure distribution over an airfoil IISct, Thiruvananthapuram, Kerala, 695547,India.
- [2]. Eastman N. Jacobs and Robert M. Pinkerton Pressure distribution over a symmetrical airfoil section with trailing edge flap Report No. 360, National Advisory Committee For Aeronautics,1930.
- [3]. Geogrey DeSena, Pressure distribution over an airfoil United States Naval Academy,Annapolis, Maryland,2012.
- [4]. Measurement of Pressure Distribution and Lift for an Airfoil Mechanics of Fluids and Transfer Processes Laboratory Experiment #3 <https://user.engineering.uiowa.edu/~cfdf/pdfs/57-020/lab4.pdf> .
- [5]. Pressure coefficient distribution on airfoil [http://www.ingaero.uniroma1.it/attachments/461\\_lect9.pdf](http://www.ingaero.uniroma1.it/attachments/461_lect9.pdf)